# G-Protein signaling increases germline stem cell activity in *Drosophila* males in response to multiple rounds of mating

Manashree Malpe*[,1,#], Leon McSwain*[,2], Chun Ng*[,1], Karl Kudyba*[,1], Jennie Nicholson[1], Maximilian Brady[1], Benjamin Parrott[3], Vinay Choksi[4], Alicia Hudson[1], and Cordula Schulz[1]

[1] Department of Cellular Biology, University of Georgia, Athens GA 30602, USA

[2] Winship Cancer Institute, Emory University, Atlanta, GA 30322, USA

[3] Odum School of Ecology, University of Georgia, Athens, GA 30602, USA

[4] School of Medicine, Duke University, Durham, NC 27708, USA

# Corresponding author: msmalpe@uga.edu

## Abstract

Though adult tissues are maintained by homeostasis, little is known about how their precursor cells adjust to a demand for specialized cells to account for changes during development or in the environment. In the male gonad, the ability to respond to a demand for increased gamete production, commonly referred to as reproductive plasticity, is essential for the fitness of an individual and the species.

Here, we show that a demand for sperm, caused by repeated male mating, increased germline stem cell (GSC) division frequency and the production of gametes. The increase in GSC divisions depended on activity of four classical G-

protein coupled receptors and downstream signaling molecules within the germline cells. Thus, GSCs are reliant on the GPCR stimulus. Among the signaling molecules, Serotonin appeared sufficient to accelerate GSC divisions in non-mated males, making the highly conserved Serotonin receptors key players in the mechanism regulating tissue replenishment.

## Introduction

Metazoan tissues undergo homeostasis wherein stem cells divide and their daughter cells proliferate and differentiate to replace lost cells. The human hematopoietic system, for example, renew a remarkable number of about one trillion blood cells per day (Dancey et al., 1976; Erslev, 1983). Stem cells and their daughters have to maintain a baseline mitotic activity for the production of daughter cells that account for the daily turnover of differentiated cells. However, whether they can modulate their mitotic activity in response to demands that challenge the system is not fully explored. In some instances, stem cells respond to physiological cues; for example, murine hematopoietic stem cells divide more frequently during pregnancy due to increased oestrogen levels (Nakada et al., 2014). In *Drosophila melanogaster*, intestinal stem cells initiate extra cell divisions upon ablation of differentiated gut cells (Amcheslavsky et al., 2009). *Drosophila* GSCs modulate their mitotic activity in response to environmental conditions, such as nutrient availability and temperature (Hsu et al., 2008; McLeod et al., 2010; Parrott et al., 2012).

Specifically, how the gonad maintains gamete production has become of increasing interest to ecology, evolution, and medicine. Recent studies on human fecundity revealed an alarming decrease in sperm numbers, specifically in western males (Levine et al., 2017). Studies in model organism have shown that fecundity can be modified by life-history traits. For example, when the field cricket (*Teleogryllus oceanicus*) is exposed to acoustic sexual signals during juvenile stages, it develops more reproductive tissue compared to its siblings kept in a silent environment (Bailey et al., 2010). In other species, including beetles and moths, researchers correlated testis size, the quality of the ejaculate, and the success to compete for mating with nutritional stress (Gage and Cook, 1994; Knell and Simmons, 2010; Perry and Rowe, 2010; Simmons, 2012).

It appears that many species have evolved strategies to adjust mating behavior and sperm production to their socio-sexual environment. For example, insects can sense the presence of rival males and dependent on it modify mating behavior, and size and quality of ejaculate (Montrose et al., 2008; Bretman et al., 2011; Tuni et al., 2016). Likewise, frogs and birds show plasticity in their ejaculate dependent on the number of other males in the colony (Dziminski et al., 2010; Pitcher et al., 2005). Though these studies have shown that males from many species show plasticity with respect to the size or quality of their ejaculate, the mechanisms and molecules that increase gamete production in response to a demand are yet to be explored.

In *Drosophila melanogaster*, a plethora of genetic tools are available that allow for manipulating and monitoring gametogenesis. The small size of the fly,

the short generation cycle, and the fairly low costs covering their maintenance allow for high throughput screens. Here, we subjected several thousand male and several million virgin female flies to mating experiments, a task that is challenging if not impossible to perform with vertebrate model organisms.

We show that males that underwent multiple rounds of mating had an increase in stem cell activity and produced more gametes compared to non-mated males. Reducing the expression of four G-protein coupled receptors (GPCRs) via RNA-Interference (RNA*i*) from the germline cells eliminated the ability of males to accelerate their GSC divisions when mated. These were the Serotonin (5-HT) Receptors 1A, 1B and 7, and the Octopamineβ2-Receptor (Octβ2R).

GPCRs constitute a large family of conserved cell surface receptors that mediate the cell's response to a wide range of external stimuli, including odors, pheromones, hormones, and neurotransmitters. Loss of GPCR signaling affects the mammalian immune response and digestive processes, and is associated with a plethora of conditions, varying from anxiety to Usher syndrome (Schoneberg et al., 2004; Wettschureck and Offermanns, 2005). Most of our understanding of how GPCRs affects development and cellular function is derived from their roles in the nervous system, such as in olfaction, memory formation, aggression, and mating behavior (Alekseyenko et al., 2014; Dacks et al., 2009; Lee et al., 2011; Pooryasin and Fiala, 2015). Only a few studies are available that describe non-neural roles of GPCRs in model organisms. In *Drosophila*, GPCRs regulate cell shape and adhesion during embryogenesis

(Manning et al., 2013; Patel et al., 2016). Zebrafish GPCR signaling regulates the development of the myelin sheath of Schwann cells around the axons and, in C. elegans, GPCR signaling aligns the neuroblasts during development (Langenhan et al., 2009; Monk et al., 2009). A number of studies, using mammalian cultured cells, show that GPCR signaling can cross-talk with effectors of the cell cycle, suggesting essential roles for GPCR signaling in development, tissue homeostasis, and cancer progression (New and Wong, 2007). However, the impacts of GPCRs on the frequency of stem cell divisions and gamete production, and how these associate with normal development and disease are yet to be explored. Our data demonstrate a novel, non-neural function for GPCR signaling, the regulation of stem cell activity.

Octβ2R and the 5-HT receptors are highly conserved and found throughout the animal kingdom (Delgado and Moreno, 2000). In mammals, 5-HT signaling is associated with reward behavior and neural malfunctions, and the vertebrate homologue of Octopamine (OA), Norepinephrine, is associated with depression (Delgado and Moreno, 2000; Hayes and Greenshaw, 2011; Popova, 2006; Schoneberg et al., 2004). The role of these conserved signaling molecules in regulating GSC activity in *Drosophila* suggests parallel roles for them and potential other GPCRs in the regulation of stem cell activity and in reproductive plasticity in other species.

## Results

### *Mating increased the number of GSCs in mitosis*

To uncover a potential mechanism for an increased production of specialized cells, we challenged *Drosophila* males via mating experiments. For each experiment, 80-100 males were exposed individually in mating chambers (Figure S1A) to three virgin females each day in a three day-long mating experiment. An equal number of male siblings were each kept in solitude and served as the non-mated controls. Mating success was investigated by two criteria: visual observation and the presence of progeny. When flies were anesthetized to exchange the females for fresh virgins, several copulating pairs of males and females were normally observed. Furthermore, 100 of the mated females were individually placed into food vials and mating success was evaluated a few days later by counting the percentage of vials with progeny. With very few exceptions, males in this study sired progeny with 60-90% of the females exposed to them on day one of the mating experiment (Table 1).

*Drosophila* gametogenesis is strikingly similar to tissue homeostasis in other metazoan species. As is typical for many stem cells, the *Drosophila* GSCs are found in a specific cellular microenvironment. Male GSCs are located at the tip of the gonad, attached to somatic hub cells (Figure 1A, A'). Upon GSC division, one of the daughter cells, called a gonialblast, undergoes four rounds of characteristic transit amplifying divisions, resulting in 16 spermatogonia. Subsequently, spermatogonia enter a tissue-specific differentiation process. They grow in size, undergo the two rounds of meiosis, and develop through extensive morphological changes into elongated spermatids (Fuller, 1993). Due

to this tightly controlled homeostasis program, each GSC division normally produces 64 spermatids (Figure 1A).

Classically, three mechanisms for how males increase gamete production can be envisioned. They could 1) increase the numbers of GSCs, and/or 2) the numbers of GSC divisions, and/or 3) the number of transit amplifying divisions (Kaczmarczyk and Kopp, 2010; Ramm and Scharer, 2014). To investigate the numbers of GSCs and their progeny we used an established immuno-fluorescence protocol (Parrott et al., 2012). We identified Vasa-positive GSCs based on their position next to FasciclinIII (FasIII)-positive hub cells (Figure 1A'). Only cells that were outlined by Vasa staining and that were clearly attached to the hub were counted as GSCs.

According to the literature, an adult male gonad contains an average of eight to ten GSCs (Chen et al., 2017; Yamashita et al., 2003). Surprisingly, we found a large variation in GSC numbers among our different fly lines. Overall, the distribution of GSCs ranged widely from one to 14 per testis, with an average of seven GSCs per testis. Males from an isogenized *wt* stock, *Oregon R* (*OR*), had the lowest average number of GSCs, having only four to five GSCs per testis. Males from another isogenized *wt* stock*, Canton S* (*CS),* had an average of six GSCs per testis. Animals mutant for *white* (*w*) alleles, $w^{1118}$ and $w^{1}$, which are commonly used as control animals and as genetic background for transgenes, had on average eight and seven GSCs per testis, respectively. Males from a *vermillion*$^{1}$*, yellow*$^{1}$ ($v^{1}$, $y^{1}$) stock, which serves as the genetic background for many RNA*i*-lines, had the highest average number of GSCs, at 11 GSCs per

testis. When mated, we did not observe a significant difference in the numbers of GSCs compared to their non-mated siblings in either of these fly stocks (Figure S1B-F).

To investigate an increase in GSC mitotic activity, we added an antibody against phosphorylated Histone-H3 (pHH3) to our immuno-fluorescent procedure. The percentage of GSCs in mitosis, the GSC M-phase index ($MI^{GSC}$) was then calculated by dividing the number of pHH3-positive GSCs by the total number of GSCs. We discovered that mated *wt* males had a significantly higher $MI^{GSC}$ compared to their non-mated siblings. The box plot in Figure 1B shows the difference in $MI^{GSC}$ between non-mated and mated populations of males from 17 independent, but tightly controlled mating experiments (see Material and Methods) using an isogenized stock of *OR* males. The $MI^{GSC}$ of non-mated males ranged from six to nine percent, with a median at seven percent. The $MI^{GSC}$ of mated males ranged from 11 to 18 percent, with a median at 16.5 percent. Even though the baseline $MI^{GSC}$ differed between individual experiments the $MI^{GSC}$ of mated males was always significantly higher than the $MI^{GSC}$ of non-mated males. We conclude that the increase in $MI^{GSC}$ of *OR* males in response to mating is highly reproducible.

We next investigated if only a few males within a population contributed to the increase in $MI^{GSC}$ or whether the effect of mating is reflected by changes in the $MI^{GSC}$ across a population. These data and the raw data in the supplemental figures are displayed in frequency distribution graphs (FDGs). FDGs show how often a particular value ($MI^{GSC}$) is represented in a population (number of testes).

When the distribution of the $MI^{GSC}$ for testes within one population of *OR* flies was plotted, the resulting FDG revealed that mated males had fewer testes with an $MI^{GSC}$ of zero and more testes with higher $MI^{GSC}$ compared to non-mated siblings (Figure 1C). The same result was obtained using *CS* males (Figure S1G). We conclude that mating affects the $MI^{GSC}$ of many males within one mated population.

Finally, we wanted to explore how many mating events it takes for the increase in $MI^{GSC}$ to occur. When we exposed *OR* males to either one or two female virgins for 24 hours, no difference in $MI^{GSC}$ between non-mated and mated males was apparent (Figure 1D, "1F, 24 hrs" and "2F, 24 hrs"). Mating *OR* males to three virgin females for 24 hours sometimes, but not always elicited an increase in $MI^{GSC}$ upon mating (Figure 1D, 3F, 24hrs). Robust and reproducible increases were seen in *OR* males that were mated to three virgin females on each of two or three days of mating (Figure 1D, "2x3F, 48 hrs" and "3x3F, 72 hrs"). The increase in $MI^{GSC}$ in mated males was reversible, showing that the response to mating was dynamic. Moving males back into solitude after the three-day mating experiment for 48 hours eliminated the increase in $MI^{GSC}$ (Figure 1D, "3x3F, 120 hrs"). Control males mated for 120 hours, in contrast, still had a significant increase in $MI^{GSC}$ (Figure 1D, "5x3F, 120 hrs").

***Mating increased GSC division frequency***

An increase in $MI^{GSC}$ could be due to an extended M-phase or to an increased division frequency. As another measure of cell divisions, we investigated the

percentage of GSCs in synthesis phase (S-phase) of the cell cycle. Testes were labeled with 5-ethynyl-2'-deoxyuridine (EdU) and the S-phase index of the GSCs ($SI^{GSC}$) was calculated by dividing the number of EdU-positive GSCs by the total number of GSCs. Using pulse-labeling experiments, we observed that mated *OR* males displayed significantly higher $SI^{GSC}$ compared to their non-mated siblings (Figure 1E). Together with the increase in the $MI^{GSC}$ this suggests that mating accelerates GSC divisions. To test this hypothesis, the lengths of the cell cycle of non-mated and mated males were compared using EdU feeding experiments. In this approach, *OR* animals were fed EdU during the mating experiment. We then calculated how many GSCs had been in S-phase at different time points. Our EdU-incorporation experiment revealed that the number of EdU-positive GSCs increased rapidly after 24 hours of feeding (Figure 1F). At 36 and 48 hours of mating, mated males had significantly more EdU-positive GSCs compared to their non-mated siblings (Figure 1F). This shows that, in mated males, more GSCs had progressed through the S-phase of the cell cycle. By 60 hours of feeding, the numbers of EdU-positive GSCs reached a plateau at which a significant difference in $SI^{GSC}$ between non-mated and mated males was no longer seen (Figure 1F). At this time, more than 80% of the GSCs were EdU-positive. Prolonged feeding did increase the percentage of EdU-positive GSCs but these data were excluded because many of the males died when fed EdU for more than three days while mating. Our EdU-feeding experiments produced a different reaction curve compared to reactions curves obtained from other studies where animals were fed the thymidine analogue, bromo-deoxy-uridine

(Wallenfang et al., 2006; Yang and Yamashita, 2015). This is probably because we used a much lower dose of a thymidine analogue.

We next tried to investigate which stage of the cell cycle is shortened upon mating using Fly-FUCCI in combination with the UAS/Gal4-expression system (Duffy, 2002; Zielke et al., 2014). With Fly-FUCCI, the coding regions of fluorescent proteins are fused to the destruction boxes of cell cycle regulators, allowing the marking of different cell cycle stages. These artificial proteins are under control of the yeast upstream activating sequences (UAS) and can be expressed in a tissue-specific manner using a variety of available Gal4-transactivators. In our case, we used a *nanos-Gal4*-transactivator (NG4) with a reported expression in GSCs, gonialblasts, and spermatogonia (Van Doren, 1998). Using two independent FUCCI-lines, we observed that $MI^{GSC}$ did not significantly increase upon mating. While mated *UAS-FUCCI/NG4* males had an $MI^{GSC}$ of 4.7% (number of GSCs=1017) their non-mated siblings had a $MI^{GSC}$ of 3.7% (number of GSCs=1281). We conclude that expressing FUCCI-constructs from these fly lines within the GSCs interfered with their ability to significantly increase $MI^{GSC}$ in response to mating. This could be because the high expression of proteins with destruction boxes may have overloaded the cell cycle machinery.

***Mating also increased the MI of gonialblasts, spermatogonia, and somatic stem* cells**

The development of a mature sperm from one GSC daughter takes nine to 11 days (Fuller 1993, Lindsley and Tokuyasu, 1980). However, it only takes a few

days for a cell to develop from a GSC through the gonialblast stage and into spermatogonial stage. Thus, three days of mating should increase the number of these early-stage germline cells (EGCs). Due to the three-dimensional arrangement of the germline cells within the testes, it is extremely challenging to reliably count the total numbers of EGCs. As another way of histological sampling we aimed towards using a single focal plane of the apical testis region. To establish the feasibility, we used GSC numbers as our control. Due to the GSC position next to the hub, they can easily be identified in both ways, in a single focal plane and in all focal planes throughout the apical tip of the testis.

After imaging the apical regions of *OR* testes (Figure 2A, A') we counted the numbers of GSC in all focal planes and, as expected, did not detect a difference between non-mated and mated males (Figure 2B, total GSCs). Using the same images, we chose a single focal plane. To avoid any bias we always picked the focal plane in which the hub is clearly seen (Figure 2A, A’, arrow). A careful analysis of these single focal plane images confirmed equal numbers of GSC in the testes of non-mated and mated *OR* males (Figure 2B, focal GSCs). This shows that using a single focal plane for analyzing a difference in GSC numbers is as informative as analyzing all focal planes. Using the same single focal plane images, we counted the numbers of EGCs. We discovered that the number of EGCs was significantly higher in the mated males compared to the non-mated males (19.5 to 23.3 EGCs per testis, Figure 2B, focal EGCs). We conclude that mating does not affect GSC numbers but does increase the production of EGCs that will eventually differentiate into sperm cells.

Having established that this histological method is reliable, we wondered if mating also increases the MI of the EGCs. Going back to the same images, we now counted the percentage of GSCs in division using both, all focal planes and only the single focal plane. In both cases, $MI^{GSC}$ was significantly increased in mated *OR* males (Figure 2C, “total GSCs” and “focal GSCs”). $MI^{EGC}$ was also increased in mated males compared to their non-mated siblings (Figure 2C, “focal EGCs”). When we used the same tissues as above to count the clusters of spermatocytes that were in meiosis, we did not detect a significant difference between non-mated and mated males. In both cases, we detected 0.8 - 0.9 meiotic clusters per testis (number of testes=100). This shows that the meiotic activity does not change in response to mating.

Somatic stem cells in the male gonad, however, did increase their MI in response to mating. In mammals and *Drosophila*, germline development depends on somatic support cells (Zoller and Schulz, 2012). Each *Drosophila* male GSC is enclosed by two Cyst Stem Cells (CySC) that are also arranged around and attached to the hub cells (Hardy et al., 1979). CySCs self-renew and produce cyst cells. Two cyst cells associate with and grow around one gonialblast to form the cellular microenvironment for the developing germline cells (Gonczy and DiNardo, 1996; Sarkar et al., 2007). Loss of germline enclosure by these somatic cells increases GSC division frequency and causes germline tumors (Parrott et al., 2012; Schulz et al., 2002). To explore CySC divisions we used the same immuno-fluorescence protocol as above but replaced the germline marker, Vasa, with the soma marker, Traffic Jam (Tj). We

then investigated those Tj-positive cells within three cell diameters away from the hub as the potential CySCs. The mitotic index of the CySCs ($MI^{CySC}$) was significantly higher in mated *OR* males than in their non-mated siblings (Figure 2D) and this increase in $MI^{CySC}$ affected the whole population of males (Figure 2E). Our data indicate that mating increases the MI of all mitotically active cells in the male gonad. However, for technical and simplicity reasons, we focus on the activity of the GSCs in the remainder of this manuscript.

***RNAi against classical GPCRs blocked the increase in $MI^{GSC}$ upon mating***

*Drosophila* mating is a complex and genetically controlled behavior that is dependent on neural circuits (Manoli et al., 2013). This implicates a possible neuronal control in regulating GSC divisions in response to mating. Thus, we focused on the type of signaling pathway commonly stimulated during neural activity, GPCR signaling (Geppetti et al., 2015). The functions of many GPCRs have not been studied yet and mutant alleles are only available in rare cases. However, collections of RNA*i*-lines that target GPCRs (*GPCR-i*) are available that are expressed under control of UAS.

A genetic screen revealed that expressing RNA*i*-constructs against four GPCRs, 5-HT1A, 5-HT1B, 5-HT7, and Octβ2R clearly and reproducibly eliminated the increase in $MI^{GSC}$ in mated males. Animals from the *GPCR-i*-lines were crossed to *wt* and two separate NG4 transactivators, *NG4-1* or *NG4-2*, and the $MI^{GSC}$ of their progeny investigated. Each of the control progeny (*GPCR-i/wt*) consistently increased their $MI^{GSC}$ when mated to females (Figure 3A and Figure

S2A-D). However, the experimental progeny, *GPCR-i/NG4-1* (Figure 3B and Figure S2E-H) and *GPCR-i/ NG4-2* (Figure 3C and Figure S2I-L), showed no significant increase in $MI^{GSC}$ in mated males across at least three replicate experiments.

Among these experiments, the $MI^{GSC}$ between different genotypes fluctuated widely. When comparing the $MI^{GSC}$ of non-mated males (blue bars) in Figure 3A to 3B and 3C, it is apparent that each of the *GPCR-i*-lines had a different baseline $MI^{GSC}$ dependent on the genetic background. These baseline $MI^{GSC}$ fall into the same range as the baseline $MI^{GSC}$ of *OR* males (compare the blue bars in Figure 3 to the blue box in Figure 1B). Furthermore, the $MI^{GSC}$ of the mated control males (*GPCR-i/wt*, red bars in Figure 3A) fall within the range of mated *OR* males (red box in Figure 1B). However, the $MI^{GSC}$ of the mated experimental males (*GPCR-i/NG4*, red bars in Figures 3B and 3C) generally remain within the range of $MI^{GSC}$ of non-mated *OR* males (blue box in Figure 1B). This confirms that the four GPCRs are required for the increase in $MI^{GSC}$ in response to mating.

Each of the genotypes produced offspring (Table 1), showing that a block in the increase in $MI^{GSC}$ is not caused by a failure to mate but by a reduction of GPCR signaling. Viable alleles of *5-HT1A* and *5-HT1B* are available, but unfortunately, displayed only a weak mating success rate and were, therefore, not pursued as alternative strategies.

***Signal transducers downstream of GPCRs were required for the increase in MI$^{GSC}$ upon mating***

To further validate that MI$^{GSC}$ is regulated by GPCR stimulation, we manipulated downstream signal transducers. Classical GPCRs associate with trimeric complexes of the G-proteins, $G_\alpha$, $G_\beta$, and $G_\gamma$ (Figure 4A, step 1). Ligand binding leads to activation of a guanidyl exchange factor within the GPCR that then exchanges GDP for GTP in the $G_\alpha$ subunit. The exchange leads to the dissociation of $G_\alpha$ and the $G_{\beta/\gamma}$ complex from each other and from the GPCR. Remaining attached to the membrane, $G_\alpha$ and $G_{\beta/\gamma}$ diffuse along it and activate downstream signal transducers (Figure 4A, step 2; McCudden et al., 2005; Oldham and Hamm, 2008). Most organisms have multiple genes that encode for each of the G-protein subunits. *Drosophila* has six $G_\alpha$, three $G_\beta$, and two $G_\gamma$-proteins, yet only a few examples are available in the literature associating a specific G-protein with an upstream GPCR (Boto et al., 2010; McCudden et al., 2005).

As mutant alleles for most G-protein subunits are lethal, we continued to use the UAS/Gal4-system. We expressed RNA*i* against the different G-protein subunits within the germline cells via *NG4-1*. Consistent with a role for several GPCRs in regulating MI$^{GSC}$, mated males expressing RNA*i* for several of the G-protein subunits displayed only a weak increase in MI$^{GSC}$ compared to their non-mated siblings (data not shown). We focused on an RNA*i*-line directed against the subunit *$G_\alpha i$* as males expressing this construct within the germline did not show any increase in MI$^{GSC}$ in response to mating. As before each of the

following experiments were performed in at least three replicates. Each population of control males (*NG4-1/wt*, *NG4-2/wt, $G_{\alpha}$i-i/wt*) displayed a significant increase in $MI^{GSC}$ when mated (Figure 4B and Figure S3A-C). Experimental males expressing *$G_{\alpha}$i-i* via *NG4-1* or *NG4-2*, however, failed to increase $MI^{GSC}$ (Figure 4C and Figure S3E, F). We next sought to validate the role for G-proteins in $MI^{GSC}$ by an alternative approach to RNA*i*. A dominant negative version of *Drosophila* $G_{\gamma}1$ ($dnG_{\gamma}1$) is available that serves as a reliable tool to abolish G-protein signaling (Deshpande et al., 2009). Males expressing *$dnG_{\gamma}1$* via either *NG4-1* or *NG4-2* never showed an increase in $MI^{GSC}$ in response to mating (Figure 4C and Figure S3G, H). Control *$dnG_{\gamma}1$/wt* animals, on the other hand, had increased $MI^{GSC}$ upon mating in every independent experiment (Figure 4B and Figure S3D).

In mammalian cells, three major G-protein-dependent signaling cascades have been described (Figure 4, steps 3a, b, c; Geppetti et al., 2015; Moolenaar, 1991). For *Drosophila*, the literature provides little information on the signaling cascades downstream of GPCRs but it is generally assumed that the mammalian signal transducers are conserved in flies. To further validate that an increase in $MI^{GSC}$ upon mating is regulated by G-protein signaling, we reduced the expression of a conserved signal transducer for which three independent RNA*i*-lines were available, *Protein Kinase C 98E* (*PKC98E*). As expected, *PKC98E-i/NG4-1* males did not show a significantly increase in $MI^{GSC}$ in response to mating for any of the three RNA*i*-lines, while a control *PKC98E $^{35275}$/wt* did respond normally (Figure 4D).

***5-HT was sufficient to significantly increase the MI$^{GSC}$***

To address potential contributions of the GPCRs to the increase in MI$^{GSC}$ in mated males we aimed towards modifying the expression levels of their ligands in non-mated males. Based on the nature of the GPCRs regulating the increase in GSC mitotic activity, the ligands are likely 5-HT and Octopamine (OA), both amines known to be produced by neurons (Maqueira et al., 2005; Saudou et al., 1992; Alekseyenko et al., 2010). Two commonly used *Gal4*-transactivators allow for stimulating those neurons that express enzymes for 5-HT synthesis, *Trh-Gal4* and *Ddc-Gal4* (Alekseyenko et al., 2014; Coleman and Neckameyer, 2005; Li et al., 2000). The neurons can be hyper-stimulated by expressing the *Drosophila* Transient Receptor Potential (TRP) channel (Sakai et al., 2009). Animals expressing *UAS-TrpA* under control of *Trh-Gal4* and *Ddc-Gal4* should release 5-HT when shifted to high temperatures, however, the amount of released 5-HT has not been evaluated for this system. Modulating 5-HT levels using this genetic tool led to the published behavioral defects but did not reveal a significant increase in MI$^{GSC}$ between non-shifted and shifted *Trh-Gal4/UAS-TrpA* or *Ddc-Gal4/UAS-TrpA* males compared to controls (*Trh-Gal4/wt* and *Ddc-Gal4/wt*; Figure 5A).

We therefore sought to control ligand concentrations more tightly using feeding experiments. 5-HT and OA are commercially available and were previously successfully fed to adult animals to study changes in their behavior. In these experiments, 1-100mM of 5-HT and 30-70µM of OA evoked behavioral

responses (Crocker and Sehgal, 2008; Majeed et al., 2014; Sujkowski et al., 2017; Willard et al., 2006). We did observed these behavioral responses when animals were fed these concentrations, but no increase in $MI^{GSC}$ was apparent. When we fed *OR* males lower concentrations of 5-HT, we observed significant increases in $MI^{GSC}$ between 60μM and 100μM (Figure 5B and Figure S4B-D). Males fed 75μM 5-HT had an $MI^{GSC}$ of 17%, which is more than a two-fold increase compared to controls. We conclude that 5-HT is sufficient to increase $MI^{GSC}$. Males fed even lower concentrations of 5-HT did not show an increase in $MI^{GSC}$ (Figure 5B, S4A). Thus, we have established a response curve of the GSCs to concentrations of 5-HT.

In contrast, when we fed OA to *OR* males in concentrations ranging from 1nM to 100μM no drastic effect on $MI^{GSC}$ was observed (Figure 5C and Figure S4E, F). We detected a small but not significant increase in $MI^{GSC}$ at 1μM. The GSCs of these males had a $MI^{GSC}$ of nine, which still falls within the upper range of the $MI^{GSC}$ seen in non-mated *OR* males (compare Figure 4C to the box plots in Figure 1B). Furthermore, we did not detect a dose-dependent response from nearby concentrations. This indicates that OA is not individually sufficient to increase $MI^{GSC}$ in adult males similar to the increase seen in mated males.

***Repeated mating and 5HT modulated the sperm pool***

To show further experimental proof of biological relevance for the increase in mitotic divisions we asked if mating produces a demand for sperm. Counting all of the individual sperm cells within a *Drosophila* testis poses extreme challenges.

Therefore, we used a Don Juan-Green Fluorescent Protein (DJ-GFP) reporter to access the overall amount of sperm within the gonads (Santel et al., 1997). With this reporter, individualized mature sperm was seen within the seminal vesicle of the male reproductive tract (Figure 6A, arrow). Based on the size and the fluorescence of the seminal vesicles, we sorted the testes into two classes. Class I testes had wide and very bright GFP-positive seminal vesicles (Figure 6A, A') and class II testes had thinner and less bright GFP-positive seminal vesicles (Figure 6B-C'). A quantification of these classes of testes revealed that non-mated males had mostly class I testes (Figure 6D, "DJ-GFP, n-m"), while mated males had mostly class II testes (Figure 6D, "DJ-GPF, m").

After mating, the GPF-positive sperm is detectable in the female reproductive tract. While non-mated females never had GFP-expression in their reproductive tracts (Figure 6E, E', n=100), mated females clearly showed GFP in the spermathecae and the seminal receptacles (Figure 6F, F', arrows and arrowhead). The percentage of female reproductive tracts that contained GFP-positive sperm at day three of the mating procedure dropped down to 25% compared to 94% in the reproductive tracts of day one females (Figure 6G). Together with the reduction of GFP in the mated male seminal vesicles, this shows that repeated mating reduced the amount of sperm available for transfer to the female. Thus, repeated mating has to create a demand for sperm.

We next asked if an increase in mitotic divisions of the precursor cells leads to more sperm production. Unfortunately, males do not survive the 11 days of mating necessary to ask if increased mitotic divisions produce more sperm.

Therefore, we used 5-HT-feeding in combination with mating to investigate an increase in sperm replenishment. In this experiment, we first fed DJ-GFP males either yeast-paste or yeast-paste supplemented with 75μM 5-T for 8 days. Then we exposed all of them to a three-day mating experiment to reduce their sperm pool. Subsequently, males were dissected at 0, 24, and 48 hours after the mating experiment and the overall amount of GFP-positive sperm in their seminal vesicles investigated. 90% of the yeast-fed males had type II testes immediately after mating and this number decreased to 64% after 48 hours (Figure 6D, "*DJ-GFP/wt*, yeast-fed"). 5-HT-fed males in contrast had only 65% of type II testes immediately after mating (Figure 6D, "*DJ-GFP/wt*, 5-HT-fed"). By 48 hours after mating, 5-HT-fed males had regained more type I than type II testes (Figure 6D, "*DJ-GFP/wt*, 5-HT-fed") By this time, 66% of the testes were of type I, and 34% of the testes were of type II. This experiments shows that increased mitotic divisions leads to expedited tissue replenishment.

## Discussion

Previous studies in *Drosophila* showed that testis size, the numbers of sperm within the male gonad, and the size and quality of the ejaculate increased in the presence of rival males (Garbazewska et al., 2013; Lupold et al., 2011; Moatt et al., 2014; Pitnick et al., 2001). Though these studies suggest an increase in spermatogenic activity in response to the socio-sexual environment, the cellular events that lead to increased sperm production were not addressed. Here, we created a demand for sperm by repeatedly mating single males with multiple

female virgins. We show that germline cells in these mated males have increased mitotic activity and produced more gametes (EGCs and sperm) compared to their non-mated siblings. We further show that this increase in spermatogenic activity depended on G-protein signaling.

Using highly controlled experiments, we demonstrate that reducing the expression or modulating the activity of GPCRs, G-proteins, or PKC98E from the germline interfered with the male GSC response to mating. Our studies revealed that at least four GPCRs are essential in mated males for the increase of $MI^{GSC}$ in response to mating. It is surprising that several GPCRs are required for the increase in $MI^{GSC}$ in mated males instead of a single GPCR. It is not likely that the RNA*i*-lines produced phenotypes due to off-target effects as their hairpins are extremely short. Rather, our finding suggests a complexity of signaling events for the regulation of GSC activity. If the four GPCRs act independently it is hard to explain how the loss of one GPCR completely blocks the increase in $MI^{GSC}$. Thus, they have to act in a non-redundant manner. This has to be mechanistically different from situations where only one or two receptors regulate a cellular or developmental process. Examples for two receptors regulating the same process have been described for several model organisms. In *Drosophila*, for example, signaling via Hedgehog and Jak/STAT (Janus Kinase signal transducer and activators of transcription) from the hub cells regulate CySC self-renewal through independent signaling cascades (Amoyel et al., 2013). In *C. elegans,* two Octopamine receptors, SER-3 and SER-6, additively regulate the same signal transducers for food-deprived-mediated signaling (Yoshida et al., 2014).

Studies on mammalian GPCRs have revealed increasing evidence that they can form dimers and oligomers and that these physical associations have a variety of functional roles, ranging from GPCR trafficking to modification of G-protein mediated signaling (Filizola and Weinstein, 2005; Milligan, 2007; Terrillon and Bouvier, 2004). Specifically, 5-HT receptors can form homo-dimers and hetero-dimers and, dependent on this, they have different effects on G-protein signaling (Herrick-Davis, 2013; Lukasiewicz et al., 2010; Xie et al., 1999). In cultured fibroblast cells, for example, G-protein coupling is more efficient when both receptors within a 5-HT4 homo-dimer bind to agonist (Pellissier et al., 2011). In Xenopus oocytes and mouse hippocampal neurons, hetero-dimerization of 5-HT1A with 5-HT7 reduces G-protein activation compared to 5-HT1A homo-dimers. The selective association of 5-HT1A with either itself or with 5-HT7 regulates the opening of a potassium channel in the brain (Pellissier et al., 2011; Renner et al., 2012). The formation of hetero-dimers of GPCRs with other types of receptors plays a role in depression in rats and in the response to hallucinogens in mice (Borroto-Escuela et al., 2016; Moreno et al., 2011). It is possible that the regulation of $MI^{GSC}$ is emerging as the first *in vivo* example for a role of an oligomer complex.

In addition to the complexity at the level of multiple receptors, signaling cascades downstream of GPCRs or GPCR complexes could crosstalk. One signaling cascade could, for example, lead to the expression of a kinase that is activated by another cascade. Similarly, one signaling cascade could open an ion channel necessary for the activity of a protein within another signaling cascade.

In this scenario, one of the GPCR activating signaling molecules could be sufficient to increase $MI^{GSC}$ but the lack of either GPCR would result in a failure to increase $MI^{GSC}$. Consistent with this idea, we show that 5-HT feeding significantly increased $MI^{GSC}$. This suggests that 5-HT is the key ligand regulating the increase in GSC division in response to mating. One possible explanation for this is that 5-HT stimulates several GPCRs or a GPCR complex on the GSCs to accelerate GSC divisions. Alternatively, 5-HT in the fly hemolymph could cause the release of OA and/or other ligands from the fly body and act in concert with these to regulate GSC divisions. The development of an organoid culture that can be maintained for several days *in vitro* should allow us to ask more in depth questions to study this mechanism. For example, we could investigate if 5-HT alone is sufficient to increase $MI^{GSC}$ and if 5-HT acts directly on the GSC 5-HT receptors.

When we stimulated 5-HT neurons or fed animals doses of 5-HT at concentrations that evoked the reported hyper-activity we did not observe an increase in $MI^{GSC}$. This observation supports the idea that the body has to balance its resources to different functions. Allocating resources to physical activity can reduce reproductive fitness. For example, the more time and energy houbara bustards (*Chlamydotis undulata*) devote to sexual display the less sperm is detectable in their ejaculate (Preston et al., 2011). The observed hyper-activity in the *Drosophila* males preventing the increase in $MI^{GSC}$ suggests that allocating energy to hyper-activity directly impacts reproductive plasticity. A requirement for four non-redundant GPCRs regulating a post-mating effect may

have evolved because each of the GPCRs is also required to regulate important other functions, and full stimulation of one of them may pull energy away from gamete production. Maybe, even the ability of GPCRs to form complexes may have evolved in non-neural tissue to increase the signaling strength, and thus the response to small changes of circulating ligands.

**Acknowledgements**

The authors are grateful to Richard Zoller, Yue Qian, Megan Aarnio, Heather Kudyba, Jacqueline Uribe, Chidemman Ihenacho, Stefani Moore, Stephanie Andino, Sampreet Reddy, Amanda Cameron, Chederli Belongilot, Dylan Ricke, Kenneth Burgess, Amanda Redding, Erin Guillebeau, Jennifer Murphy, Chantel McCarty, Sarah Murphy, Haley Grable, Mitch Hanson, Haein Kim, and Sarah Rupert for technical assistance. We thank Bruce Baker, Carmen Robinett, Edward Kravitz, Matthew Freeman, Mark Brown, Erika Matunis, Steve DiNardo, Margaret Fuller, Allan Spradling, Hannele Rahuola-Baker, Eric Bohman, Celeste Berg, Claude Desplan, Wolfgang Lukowitz, Patricia Moore, Jim Lauderdale, Michael Tiemeyer, Scott Dougan, and Ping Shen for helpful discussions. We are especially grateful to Barry Ganetzky for the *X^X, shi* $^{ts}$ fly stock, and to Wolfgang Lukowitz for the use of his microscope. This work was supported by NSF grants #0841419 and #1355009.

**Author Contributions**

M.M., C.N., K.K., B.P., and C.S. conceived the experiments, M.M., L.M, C.N., K.K., J.N., M.B., B.P., V.C., A.H., and C.S performed the experiments, M.M., K.K., and C.S. analyzed the data, M.M. and C.S. wrote the manuscript.

**Declaration of Interests**

The authors declare no competing interests.

**References**

Alekseyenko, O.V., Y.B. Chan, M.P. Fernandez, T. Bulow, M.J. Pankratz, and E.A. Kravitz. 2014. Single serotonergic neurons that modulate aggression in Drosophila. *Curr Biol*. 24:2700-7.

Alekseyenko, O.V., C. Lee, and E.A. Kravitz. 2010. Targeted manipulation of serotonergic neurotransmission affects the escalation of aggression in adult male Drosophila melanogaster. *PLoS One*. 5:e10806.

Amcheslavsky, A.,J. Jiang, and Y.T. Ip. 2009. Tissue damage-induced intestinal stem cell division in Drosophila. *Cell Stem Cell*. 4:49-61.

Amoyel, M., J. Sanny, M. Burel, and E.A. Bach. 2013. Hedgehog is required for CySC self-renewal but does not contribute to the GSC niche in the Drosophila testis. *Development*. 140:56-65.

Bailey, N.W., B. Gray, and M. Zuk. 2010. Acoustic experience shapes alternative mating tactics and reproductive investment in male field crickets. *Curr Biol*. 20:845-9.

Borroto-Escuela, D.O., A.O. Tarakanov, and K. Fuxe. 2016. FGFR1-5-HT1A Heteroreceptor Complexes: Implications for Understanding and Treating Major Depression. *Trends Neurosci*. 39:5-15.

Boto, T., C. Gomez-Diaz, and E. Alcorta. 2010. Expression analysis of the 3 G-protein subunits, Galpha, Gbeta, and Ggamma, in the olfactory receptor organs of adult Drosophila melanogaster. *Chem Senses*. 35:183-93.

Boyle, M., C. Wong, M. Rocha, and D.L. Jones. 2007. Decline in self-renewal factors contributes to aging of the stem cell niche in the Drosophila testis. *Cell Stem Cell*. 1:470-8.

Bretman, A., M.J. Gage, and T. Chapman. 2011. Quick-change artists: male plastic behavioural responses to rivals. *Trends Ecol Evol*. 26:467-73.

Chen, D., X. Zhu, L. Zhou, J. Wang, X. Tao, S. Wang, F. Sun, X. Kan, Z. Han, and Y. Gu. 2017. Gilgamesh is required for the maintenance of germline stem cells in Drosophila testis. *Sci Rep*. 7:5737.

Chen, J., N. Turkel, N. Hemati, M.T. Fuller, A.J. Hunt, and Y.M. Yamashita. 2008. Centrosome misorientation reduces stem cell division during ageing. *Nature*. 456:599-604.

Coleman, C.M., and W.S. Neckameyer. 2005. Serotonin synthesis by two distinct enzymes in Drosophila melanogaster. *Arch Insect Biochem Physiol*. 59:12-31.

Crocker, A., and A. Sehgal. 2008. Octopamine regulates sleep in drosophila through protein kinase A-dependent mechanisms. *J Neurosci*. 28:9377-85.

Dacks, A.M., D.S. Green, C.M. Root, A.J. Nighorn, and J.W. Wang. 2009. Serotonin modulates olfactory processing in the antennal lobe of Drosophila. *J Neurogenet*. 23:366-77.

Dancey, J.T., K.A. Deubelbeiss, L.A. Harker, and C.A. Finch. 1976. Neutrophil kinetics in man. *J Clin Invest*. 58:705-15.

Delgado, P.L., and F.A. Moreno. 2000. Role of norepinephrine in depression. *J Clin Psychiatry*. 61 Suppl 1:5-12.

Deshpande, G., A. Godishala, and P. Schedl. 2009. Ggamma1, a downstream target for the hmgcr-isoprenoid biosynthetic pathway, is required for releasing the Hedgehog ligand and directing germ cell migration. *PLoS Genet*. 5:e1000333.

Duffy, J.B. 2002. GAL4 system in Drosophila: a fly geneticist's Swiss army knife. *Genesis*. 34:1-15.

Dziminski, M.A., J.D. Roberts, M. Beveerdige, and L.W. Simmons. 2010. Among-population variation between sperm competition and ejaculate expenditure in fropgs. *Behav Ecol*. 21:322-8.

Erslev, A. 1983. Production of erythrocytes. *In* Hematology. B.E. William WJ, Erslev AJ, Lichtman MA, editor. Mc-Graw-Hill, New York, NY. 365-376.

Filizola, M., and H. Weinstein. 2005. The study of G-protein coupled receptor oligomerization with computational modeling and bioinformatics. *FEBS J*. 272:2926-38.

Fuller, M.T. 1993. Spermatogenesis in *Drosophila. In* The development of *Drosophila melanogaster.* M. Bate, Martinez Arias, A., editor. Cold Spring Harbor Laboratory Press, Cold Spring Harbor, New York, USA. 71-148.

Gage, M.J.G., and P.A. Cook, 1994. Sperm size or numbers? Effects of nutritional stress upon eupyrene and apyrene sperm production strategies in the moth Plodia interpunctella (Lepidoptera: Pyralidae). *Funct. Ecol.* 8:594-9.

Garbaczewska, M., J.C. Billeter, and J.D. Levine. 2013. Drosophila melanogaster males increase the number of sperm in their ejaculate when perceiving rival males. *J Insect Physiol*. 59:306-10.

Geppetti, P., N.A. Veldhuis, T. Lieu, and N.W. Bunnett. 2015. G Protein-Coupled Receptors: Dynamic Machines for Signaling Pain and Itch. *Neuron*. 88:635-49.

Goenczy, P., and S. DiNardo. 1996. The germ line regulates somatic cyst cell proliferation and fate during Drosophila spermatogenesis. *Development*. 122:2437-47.

Hardy, R.W., K.T. Tokuyasu, D.L. Lindsley, and M. Garavito. 1979. The germinal proliferation center in the testis of Drosophila melanogaster. *J Ultrastruct Res*. 69:180-90.

Hayes, D.J., and A.J. Greenshaw. 2011. 5-HT receptors and reward-related behaviour: a review. *Neurosci Biobehav Rev*. 35:1419-49.

Herrick-Davis, K. 2013. Functional significance of serotonin receptor dimerization. *Exp Brain Res*. 230:375-86.

Hsu, H.J., L. LaFever, and D. Drummond-Barbosa. 2008. Diet controls normal and tumorous germline stem cells via insulin-dependent and -independent mechanisms in Drosophila. *Dev Biol*. 313:700-12.

Inaba, M., H. Yuan, and Y.M. Yamashita. 2011. String (Cdc25) regulates stem cell maintenance, proliferation and aging in Drosophila testis. *Development*. 138:5079-86.

Kaczmarczyk, A.N., and A. Kopp. 2010. Germline stem cell maintenance as a proximate mechanisms of life-history trade-offs? *Bioassays*. 33:5-12.

Knell, R.J., and L.W. Simmons. 2010. Mating tactics determine patterns of condition dependence in a dimorphic horned beetle. *Proc Biol Sci*. 277:2347-53.

Langenhan, T., S. Promel, L. Mestek, B. Esmaeili, H. Waller-Evans, C. Hennig, Y. Kohara, L. Avery, I. Vakonakis, R. Schnabel, and A.P. Russ. 2009. Latrophilin signaling links anterior-posterior tissue polarity and oriented cell divisions in the C. elegans embryo. *Dev Cell*. 17:494-504.

Lee, P.T., H.W. Lin, Y.H. Chang, T.F. Fu, J. Dubnau, J. Hirsh, T. Lee, and A.S. Chiang. 2011. Serotonin-mushroom body circuit modulating the formation of anesthesia-resistant memory in Drosophila. *Proc Natl Acad Sci U S A*. 108:13794-9.

Levine, H., N. Jorgensen, A. Martino-Andrade, J. Mendiola, D. Weksler-Derri, I. Mindlis, R. Pinotti, and S.H. Swan. 2017. Temporal trends in sperm count: a systematic review and meta-regression analysis. *Hum Reprod Update*. 23:646-59.

Li, H., S. Chaney, I.J. Roberts, M. Forte, and J. Hirsh. 2000. Ectopic G-protein expression in dopamine and serotonin neurons blocks cocaine sensitization in Drosophila melanogaster. *Curr Biol*. 10:211-4.

Lindsley, D.L., and Tokuyasu, K. T. 1980. Spermatogenesis. *In* Genetics and biology of Drosophila. W.T.R. M. Ashburner, editor. Academic Press, New York, USA. 225-94.

Lukasiewicz, S., A. Polit, S. Kedracka-Krok, K. Wedzony, M. Mackowiak, and M. Dziedzicka-Wasylewska. 2010. Hetero-dimerization of serotonin 5-HT(2A) and dopamine D(2) receptors. *Biochim Biophys Acta*. 1803:1347-58.

Lupold, S., J. Wistuba, O.S. Damm, J.W. Rivers, and T.R. Birkhead. 2011. Sperm competition leads to functional adaptations in avian testes to maximize sperm quantity and quality. *Reproduction*. 141:595-605.

Majeed, Z.R., A. Stacy, and R.L. Cooper. 2014. Pharmacological and genetic identification of serotonin receptor subtypes on Drosophila larval heart and aorta. *J Comp Physiol B*. 184:205-19.

Manning, A.J., K.A. Peters, M. Peifer, and S.L. Rogers. 2013. Regulation of epithelial morphogenesis by the G protein-coupled receptor mist and its ligand fog. *Sci Signal*. 6:ra98.

Manoli, D.S., P. Fan, E.J. Fraser, and N.M. Shah. 2013. Neural control of sexually dimorphic behaviors. *Curr Opin Neurobiol*. 23:330-8.

Maqueira, B., H. Chatwin, and P.D. Evans. 2005. Identification and characterization of a novel family of Drosophila beta-adrenergic-like octopamine G-protein coupled receptors. *J Neurochem*. 94:547-60.

McCudden, C.R., M.D. Hains, R.J. Kimple, D.P. Siderovski, and F.S. Willard. 2005. G-protein signaling: back to the future. *Cell Mol Life Sci*. 62:551-77.

McLeod, C.J., L. Wang, C. Wong, and D.L. Jones. 2010. Stem cell dynamics in response to nutrient availability. *Curr Biol*. 20:2100-5.

Milligan, G. 2007. G protein-coupled receptor dimerisation: molecular basis and relevance to function. *Biochim Biophys Acta*. 1768:825-35.

Moatt, J.P., C. Dytham, and M.D. Thom. 2014. Sperm production responds to perceived sperm competition risk in male Drosophila melanogaster. *Physiol Behav*. 131:111-4.

Monk, K.R., S.G. Naylor, T.D. Glenn, S. Mercurio, J.R. Perlin, C. Dominguez, C.B. Moens, and W.S. Talbot. 2009. A G protein-coupled receptor is essential for Schwann cells to initiate myelination. *Science*. 325:1402-5.

Montrose V.T, W.Edwin Harris, A.J. Moore, and P.J. Moore. 2008. Sperm competition within a dominance hierarchy: investment in social status vs. investment in ejaculates. *J. Evol. Biol.* 21:1290-6.

Moolenaar, W.H. 1991. G-protein-coupled receptors, phosphoinositide hydrolysis, and cell proliferation. *Cell Growth Differ*. 2:359-64.

Moreno, J.L., T. Holloway, L. Albizu, S.C. Sealfon, and J. Gonzalez-Maeso. 2011. Metabotropic glutamate mGlu2 receptor is necessary for the pharmacological and behavioral effects induced by hallucinogenic 5-HT2A receptor agonists. *Neurosci Lett*. 493:76-9.

Nakada, D., H. Oguro, B.P. Levi, N. Ryan, A. Kitano, Y. Saitoh, M. Takeichi, G.R. Wendt, and S.J. Morrison. 2014. Oestrogen increases haematopoietic stem-cell self-renewal in females and during pregnancy. *Nature*. 505:55-8.

New, D.C., and Y.H. Wong. 2007. Molecular mechanisms mediating the G protein-coupled receptor regulation of cell cycle progression. *J Mol Signal*. 2:2.

Oldham, W.M., and H.E. Hamm. 2008. Heterotrimeric G protein activation by G-protein-coupled receptors. *Nat Rev Mol Cell Biol*. 9:60-71.

Parrott, B.B., A. Hudson, R. Brady, and C. Schulz. 2012. Control of germline stem cell division frequency-a novel, developmentally regulated role for epidermal growth factor signaling. *PLoS One*. 7:e36460.

Patel, M.V., J.Y. Zhu, Z. Jiang, A. Richman, M.F. VanBerkum, and Z. Han. 2016. Gia/Mthl5 is an aorta specific GPCR required for Drosophila heart tube morphology and normal pericardial cell positioning. *Dev Biol*. 414:100-7.

Pitcher, T.E., P.O. Dunn, and L.A. Whittingham. 2005. Sperm competition and the evolution of testes size in birds. *J Evol Biol*. 18:557-67.

Pellissier, L.P., G. Barthet, F. Gaven, E. Cassier, E. Trinquet, J.P. Pin, P. Marin, A. Dumuis, J. Bockaert, J.L. Baneres, and S. Claeysen. 2011. G protein activation by serotonin type 4 receptor dimers: evidence that turning on two protomers is more efficient. *J Biol Chem*. 286:9985-97.

Perry, J.C., and L. Rowe, 2010. Condition-dependent ejaculate size and composition in a ladybird beetle. *Proc. R. Soc. Lond. B*. 277:3639-48.

Pitnick, S., G.T. Miller, J. Reagan, and B. Holland. 2001. Males' evolutionary response to experimental removal of sexual selection. *Proc R Soc Lond B.* 268:1071-80.

Pooryasin, A., and A. Fiala. 2015. Identified Serotonin-Releasing Neurons Induce Behavioral Quiescence and Suppress Mating in Drosophila. *J Neurosci*. 35:12792-812.

Popova, N.K. 2006. From genes to aggressive behavior: the role of serotonergic system. *Bioessays*. 28:495-503.

Preston, B.T., M.S. Jalme, Y. Hingrat, F. Lacroix, and G. Sorci. 2011. Sexually extravagant males age more rapidly. *Ecol Lett*. 14:1017-24.

Ramm, S.A., and L. Scharer. 2014. The evolutionary ecology of testicular function: size isn't everything. *Biol Rev Camb Philos Soc*. 89:874-88.

Renner, U., A. Zeug, A. Woehler, M. Niebert, A. Dityatev, G. Dityateva, N. Gorinski, D. Guseva, D. Abdel-Galil, M. Frohlich, F. Doring, E. Wischmeyer, D.W. Richter, E. Neher, and E.G. Ponimaskin. 2012. Heterodimerization of serotonin receptors 5-HT1A and 5-HT7 differentially regulates receptor signalling and trafficking. *J Cell Sci*. 125:2486-99.

Rorth, P. 1998. Gal4 in the Drosophila female germline. *Mech Dev*. 78:113-8.

Sakai, T., J. Kasuya, T. Kitamoto, and T. Aigaki. 2009. The Drosophila TRPA channel, Painless, regulates sexual receptivity in virgin females. *Genes Brain Behav*. 8:546-57.

Santel, A., T. Winhauer, N. Blumer, and R. Renkawitz-Pohl. 1997. The Drosophila don juan (dj) gene encodes a novel sperm specific protein

component characterized by an unusual domain of a repetitive amino acid motif. *Mech Dev*. 64:19-30.

Sarkar, A., N. Parikh, S.A. Hearn, M.T. Fuller, S.I. Tazuke, and C. Schulz. 2007. Antagonistic roles of Rac and Rho in organizing the germ cell microenvironment. *Curr Biol*. 17:1253-8.

Saudou, F., U. Boschert, N. Amlaiky, J.L. Plassat, and R. Hen. 1992. A family of Drosophila serotonin receptors with distinct intracellular signalling properties and expression patterns. *EMBO J*. 11:7-17.

Schoneberg, T., A. Schulz, H. Biebermann, T. Hermsdorf, H. Rompler, and K. Sangkuhl. 2004. Mutant G-protein-coupled receptors as a cause of human diseases. *Pharmacol Ther*. 104:173-206.

Schulz, C., C.G. Wood, D.L. Jones, S.I. Tazuke, and M.T. Fuller. 2002. Signaling from germ cells mediated by the rhomboid homolog stet organizes encapsulation by somatic support cells. *Development*. 129:4523-34.

Simmons, L.W. 2012. Resource allocation trade-off between sperm quality and immunity in the field cricket, Teleogryllus oceanicus. *Behav. Ecol.* 23:166-173.

Sujkowski, A., D. Ramesh, A. Brockmann, and R. Wessells. 2017. Octopamine Drives Endurance Exercise Adaptations in Drosophila. *Cell Rep*. 21:1809-23.

Terrillon, S., and M. Bouvier. 2004. Roles of G-protein-coupled receptor dimerization. *EMBO Rep*. 5:30-4.

The FlyBase Consortium, 2003. The FlyBase database of the Drosophila genome projects and community literature. *Nucleic Acids Res*. 31:172-5.

Tulina, N.M., W.F. Chen, J.H. Chen, M. Sowcik, and A. Sehgal. 2014. Day-night cycles and the sleep-promoting factor, Sleepless, affect stem cell activity in the Drosophila testis. *Proc Natl Acad Sci U S A*. 111:3026-31.

Tuni, C., J. Perdigon Ferreira, Y. Fritz, A. Munoz Meneses, and C. Casparini. 2016. Impaired sperm quality, delayed mating but no costs for offspring fitness in crickets winning a fight. *J. Evol. Biol.* 29:1643-7.

Van Doren, M., A.L. Williamson, and R. Lehmann. 1998. Regulation of zygotic gene expression in Drosophila primordial germ cells. *Curr Biol*. 8:243-6.

Wallenfang, M.R., R. Nayak, and S. DiNardo. 2006. Dynamics of the male germline stem cell population during aging of Drosophila melanogaster. *Aging Cell*. 5:297-304.

Wettschureck, N., and S. Offermanns. 2005. Mammalian G proteins and their cell type specific functions. *Physiol Rev*. 85:1159-204.

Willard, S.S., C.M. Koss, and C. Cronmiller. 2006. Chronic cocaine exposure in Drosophila: life, cell death and oogenesis. *Dev Biol*. 296:150-63.

Xie, Z., S.P. Lee, B.F. O'Dowd, and S.R. George. 1999. Serotonin 5-HT1B and 5-HT1D receptors form homodimers when expressed alone and

Yamashita, Y.M., D.L. Jones, and M.T. Fuller. 2003. Orientation of asymmetric stem cell division by the APC tumor suppressor and centrosome. *Science*. 301:1547-50.

Yang, H., and Y.M. Yamashita. 2015. The regulated elimination of transit-amplifying cells preserves tissue homeostasis during protein starvation in Drosophila testis. *Development*. 142:1756-66.

Yoshida, M., E. Oami, M. Wang, S. Ishiura, and S. Suo. 2014. Nonredundant function of two highly homologous octopamine receptors in food-deprivation-mediated signaling in Caenorhabditis elegans. *J Neurosci Res*.

Zielke, N., J. Korzelius, M. van Straaten, K. Bender, G.F. Schuhknecht, D. Dutta, J. Xiang, and B.A. Edgar. 2014. Fly-FUCCI: A versatile tool for studying cell proliferation in complex tissues. *Cell Rep*. 7:588-98.

Zoller, R., and C. Schulz. 2012. The Drosophila cyst stem cell lineage: Partners behind the scenes? *Spermatogenesis*. 2:145-57.

## Material and Methods

### *Fly husbandry*

Flies were raised on a standard cornmeal/agar diet and maintained in temperature-, light-, and humidity-controlled incubators. Unless otherwise noted, all mutations, markers, and transgenic lines are described in the Drosophila database and were obtained from the Bloomington stock center (The Flybase Consortium, 2003). Fly-FUCCI: BL#55101, BL#55110; NG4-2: BL#4937; UAS-TrpA: BL#26263; Ddc-Gal4: BL#7009; Trh-Gal4: BL#38389, UAS- $G_{\alpha}$i: BL#35407, UAS-dn$G_{\gamma}$1: 44604. Most of the RNA*i*-lines we obtained from the Bloomington stock center carry a UAS-promotor with high levels of expression in the germline cells (Rorth, 1998).

### *UAS/Gal4-expression studies*

For mating experiments, females from two separate *X; UAS-dicer; nanos-Gal4* (*NG4-1* and *NG4-2*) lines or *OR* females were crossed with males carrying target genes under the control of UAS. For neural hyper-stimulation, *OR* or *X; UAS-TrpA* females were crossed to *Trh-Gal4* and *Ddc-Gal4* males. The animals were placed into egg lay containers with fresh apple juice/agar-plates and yeast paste. Experimental or control progeny were transferred into food bottles, raised to adulthood at 18°C, and then shifted to 29°C for seven days to induce high activity of Gal4.

### *Statistical analysis*

Statistical relevance was determined using the Graphpad student's t-test. We used a more rigorous method to evaluate the P-value than most other studies did. In our experiments, we counted each GSC and based the P-value on the percentage of pHH3-positive GSCs out of the total number of GSCs. Other studies calculated the P-value based on numbers of dividing GSCs per numbers of testes (Boyle et al., 2007; Chen et al, 2008; Inaba et al., 2011; Tulina et al., 2014).

### *Male mating experiments*

Unless otherwise noted, mating experiments were performed at 29°C. Males and virgin females were placed on separate apple juice/agar-plates with yeast paste

overnight to assure they were well fed prior to their transfer into mating chambers. Single males were placed into each mating slot either by themselves (non-mated) or with virgin females (mated) and the chambers closed with apple juice/agar-lids with yeast paste. Females were replaced normally by virgin females on each of the following two days and apple juice/agar-lids with yeast paste were replaced on a daily basis for both non-mated and mated animals. Non-mated and mated animals were treated exactly the same way and always dissected in parallel at the same time of the day. Unless otherwise noted, females from the stock *X^X, y, w, f / Y / shi*$^{ts}$ were used as virgins. When raised at 29°C, only females hatch from this stock. For fertility tests, *OR* virgins were used. Note that 10-20% of the mated males died during the experiment while only 5% of the non-mated males died.

***Immuno-fluorescence and microscopy***

Animals were placed on ice to immobilize them. Gonads were dissected in Tissue Isolation Buffer (TIB) and collected in a 1.5 ml tube with TIB buffer on ice for no more than 30 minutes. Gonads were then fixed, followed by immuno-fluorescence staining and imaging as previously described (Parrott et al., 2012). The mouse anti-FasciclinIII (FasIII) antibody (1:10) developed by C. Goodman was obtained from the Developmental Studies Hybridoma Bank, created by the NICHD of the NIH and maintained at The University of Iowa, Department of Biology, Iowa City, IA 52242. Goat anti-Vasa antibody (1:50 to 1:300) was obtained from Santa Cruz Biotechnology Inc. (sc26877), rabbit anti-

phosphorylated Histone H3 (pHH3) antibodies (1:100 to 1:1000) were obtained from Fisher (PA5-17869), Milllipore (06-570), and Santa Cruz Biotechnology Inc. (sc8656-R). Guinea pig-anti-Tj antibody (1:5000) was a gift from Dorothea Godt. Secondary Alexa 488-, 568-, and 647-coupled antibodies (1:1000) and Slow Fade Gold embedding medium with DAPI were obtained from Life Technologies. Images were taken with a Zeiss Axiophot, equipped with a digital camera, an apotome, and Axiovision Rel. software. Bar graphs were produced in Adobe Photoshop, and plots and FDGs were produced in Graphpad Prism.

***EdU-labeling experiments***

The EdU-labeling kit was obtained from Invitrogen and the procedure performed following manufacturer's instructions. For EdU-pulse labeling experiments, animals were mated as described above, and the dissected testes incubated with 10mM EdU in PBS for 30 minutes at room temperature prior to fixation. For EdU-feeding experiments, sets of 100 *OR* non-mated and mated males were fed 10 μM EdU in liquid yeast provided on paper towels. These animals were kept at room temperature (21°C) because the paper towels easily dried out at higher temperatures, causing the flies to dehydrate and die.

***5-HT- and OA-feeding experiments***

*OR* males were collected at one week of age and kept separate from females for at least three days. Subsequently, groups of 100 males were exposed to yeast supplemented with varying concentration of 5-HT (Arcos Organics, #215025000)

or OA (Sigma, #O0250) on apple-juice/agar-plates at 29°C. The plates were replaced after 24 and 48 hours and males were dissected after a total of 72 hours.

## Tables and Legends

| Genotype | BL # | Male fertility |
|---|---|---|
| *OR* | N/A | 72% |
| *CS* | N/A | 62% |
| $w^{1118}$ | N/A | 81% |
| $w^{1}$ | 679 | 70% |
| *5-HT1A-i/NG4-1* | 33885 | 75% |
| *5-HT1B-i/NG4-1* | 33418 | 61% |
| *5-HT7-i/NG4-2* | 27273 | 91% |
| *Octβ2R-i/NG4-1* | 50580 | 89% |
| $5HT\text{-}1A^{\Delta 5kb}/5HT\text{-}1A^{\Delta 5kb}$ | 27640 | 15% |
| $5HT\text{-}1B^{\Delta III\text{-}V}/5HT\text{-}1B^{\Delta III\text{-}V}$ | 55846 | 30% |

**Table 1.** Fertility assay of select genotypes.

Male fertility based on the % of females that produced offspring after mating with males of the indicated genotype. BL#: Bloomington stock number.

## Figure legends

**Figure 1. Mating increased GSC division frequency.**

A) Cartoon depicting the stages of *Drosophila* spermatogenesis. Note that every GSC division produces exactly 64 spermatids. GB: gonialblast, SG: spermatogonia, SC: spermatocytes, SP: spermatids.

A') The apical tip of an *OR* testis. The FasIII-positive hub (asterix) is surrounded by Vasa-positive GSCs (arrows), one of which is in mitosis based on anti-pHH3-staining (arrowhead). Scale bar: 10μm.

B-F) Blue: non-mated condition, red: mated condition, ***: P-value < 0.001, number of GSCs as indicated.

B) Box plot showing the variability in $MI^{GSC}$ of non-mated and mated *OR* males.

C) FDG showing $MI^{GSC}$ across a population of males on the X-axis and the percentage of testes with each $MI^{GSC}$ on the Y-axis, numbers of testes (n=) as indicated.

D) Bar graph showing $MI^{GSC}$ after different mating conditions, as indicated. F: female virgins, hrs: hours, numbers of GSCs notated in bars.

E) Bar graph showing $SI^{GSC}$ of *OR* males, numbers of GSCs notated in bars.

F) Graph showing the percentage of EdU-marked *OR* GSCs on the Y-axis and hours of feeding and mating on the X-axis.

**Figure 2. Mating increase the MI of all mitotically active cells of the male gonad.**

A) The apical region of an *OR* testis showing Vasa-positive GSCs and EGCs in red, and the hub and pHH3-positive cells in green. Arrow points to the hub, scale bars: 30μm.

A') Same testis tip as in (A) showing germline cells only,

B-E) Blue: non-mated conditions, red: mated condition, ***: P-value < 0.001.

B) Bar graph showing the numbers of GSCs and EGCs in *OR* testes, numbers of testes (n=) as indicated.

C) Bar graph showing $MI^{GSC}$ and $MI^{EGC}$ in *OR* testes, numbers of GSCs are notated in bars.

D) Bar graph showing the MI of CySCs of *OR* males, numbers of CySCs notated in bars.

E) FDG showing $MI^{CySC}$ across a population of *OR* males, numbers of testes (n=) as indicated.

**Figure 3. Expression of RNA*i* against four GPCRs blocked the increase in $MI^{GSC}$ in response to mating.**

A-C) Bar graphs showing $MI^{GSC}$. Blue: non-mated condition, red: mated condition, numbers of GSCs notated in bars, genotypes as indicated, ***: P-value < 0.001. Each bar represents the $MI^{GSC}$ obtained from at least three independent experiments.

A) Control males have significantly higher $MI^{GSC}$ than their non-mated siblings.

B, C) Mated *GPCR-i/NG4-1* (B) and *GPCR-i/NG4-2* (C) did not have significantly higher $MI^{GSC}$ compared to their non-mated siblings.

**Figure 4. Signal transducers downstream of GPCRs were required for the increase in $MI^{GSC}$ in response to mating.**

A) Cartoon depicting the activation of G-proteins upon GPCR stimulation by ligand. 1: G-protein association before GPCR stimulation, 2: G-protein

distribution after GPCR stimulation, 3: potential signaling molecules modified by G-proteins.

B-D) Bar graphs. Blue: non-mated condition, red: mated condition, ***: P-value < 0.001, numbers of GSCs notated in bars, genotypes as indicated.

B) Control animals increased their $MI^{GSC}$ when mated.

C) Males expressing *Gαi-i* or *dnGγ1* in the germline did not increase $MI^{GSC}$ upon mating.

D) Bar graph showing $MI^{GSC}$ upon reduction of *PKC98E*.

**Figure 5: 5-HT was sufficient to increase $MI^{GSC}$.**

A-C) Bar graphs. Brown: $MI^{GSC}$ from control males, green: $MI^{GSC}$ from experimental males, ***: P-value < 0.001, **: P-value < 0.05, numbers of GSCs notated in bars.

A) $MI^{GSC}$ from control males and males with hyper-stimulated 5-HT neurons, genotypes as indicated.

B, C) Drug concentrations as indicated.

B) $MI^{GSC}$ in 5-HT-fed males. Note that the significant bars represent at least two independent experiments.

C) $MI^{GSC}$ in OA-fed males.

**Figure 6. Mating and 5-HT-feeding had opposite effects on the sperm pool.**

A-C') Class I and II testes from Dj-GFP males. The DNA-stain, 4',6-Diamino-2-Phenylindole (DAPI), outlines the gonads. A, B, C) DAPI and GFP, arrows point to seminal vesicles, scale bars: 30μm. A', B', C') GFP only.

D) Bar graph showing the distribution of class I (light green) and class II (dark green) testes in 1) non-mated (n-m) and mated (m) DJ-GFP males, 2) yeast-fed *DJ-GFP/wt* males at 0, 24, and 48 hours after mating, and 3) 5-HT-fed *DJ-GFP/wt* males at 0, 24, and 48 hours after mating. Numbers of testes (n=) as indicated, ***: P-value < 0.001, hrs: hours.

E-F') Female uteri with attached reproductive structures outlines by DAPI. E, F) DAPI and GFP, arrows point to spermathecae, arrowheads point to seminal receptacles, scale bars: 30μm. E', F') GFP only.

G) Bar graph showing the distribution of female reproductive tracts containing no GFP (light green) and GFP-positive sperm (mid green). Numbers of reproductive tracts (n=) as indicated, ***: P-value < 0.001.

**Supplemental figure legends**

**Figure S1. Mating did not increase GSC numbers.**

A) A mating chamber made from a box of 1ml tips. The ends of the tips were cut and a net glued onto them. The tips were then glued tight into the box. The lids were filled with apple juice/agar and covered with a layer of yeast paste.

B-G) Blue: non-mated condition, red: mated condition, numbers of testes (n=) as indicated, genotypes as indicated.

B-F) Bar graphs showing numbers of GSCs in males from different genetic backgrounds on the X-axis and the percentage of testes containing these numbers of GSCs on the Y-axis.

G) FDGs showing $MI^{GSC}$ across a population of *CS* males on the X-axis and the percentage of testes with each $MI^{GSC}$ on the Y-axis,

**Figure S2. Expression of RNA*i* against amine GPCRs blocked the increase in $MI^{GSC}$ in response to mating.**

A-U) FDGs showing $MI^{GSC}$ across a population of males on the X-axis and the percentage of testes with each $MI^{GSC}$ on the Y-axis, numbers of testes (n=) as indicated, blue: non-mated condition, red: mated condition, genotypes as indicated.

A-D) *GPCR-i/wt* males.

E-H) *GPCR-i/NG4-1* males.

I-L) *GPCR-i/NG4-2* males.

**Figure S3. G-proteins were required for the increase in $MI^{GSC}$ in response to mating.**

A-H) FDGs showing $MI^{GSC}$ across a population of males on the X-axis and the percentage of testes with each $MI^{GSC}$ on the Y-axis, numbers of testes (n=) as indicated, blue: mated condition, red: mated condition, genotypes as indicated.

A-D) Control males.

E-H) Males that express *Gαi-i* or *dnGγ1* in the germline.

**Figure S4: 5-HT was sufficient to increase $MI^{GSC}$.**

A-F) FDGs showing $MI^{GSC}$ across a population of males on the X-axis and the percentage of testes with each $MI^{GSC}$ on the Y-axis. Brown: $MI^{GSC}$ from control males, green: $MI^{GSC}$ from experimental males, number of testes (n=) as indicated, drug concentrations as indicated.

A-D) 5-HT-fed males.

E, F) OA-fed males.

## Figures

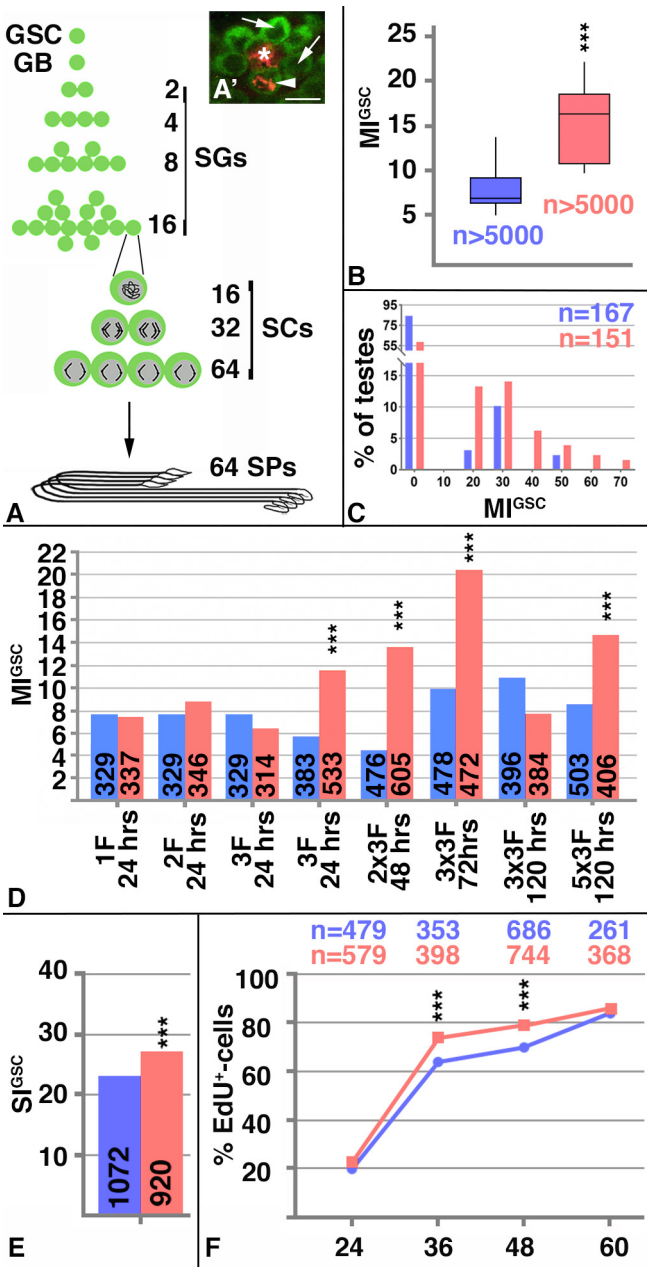


**Figure 1**

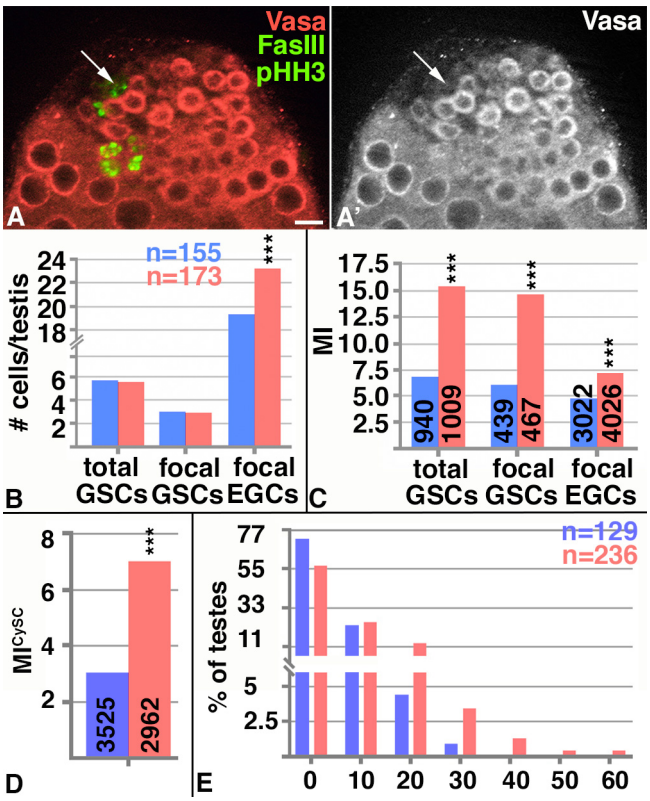
Vasa
FasIII
pHH3
A
Vasa
A'
n=155
n=173
***
# cells/testis
24
22
20
18
6
4
2
total GSCs
focal GSCs
focal EGCs
B
MI
17.5
15.0
12.5
10.0
7.5
5.0
2.5
940
1009
439
467
3022
4026
C
MI^CySC
8
6
4
2
3525
2962
D
% of testes
77
55
33
11
5
2.5
n=129
n=236
0
10
20
30
40
50
60
E

**Figure 2**

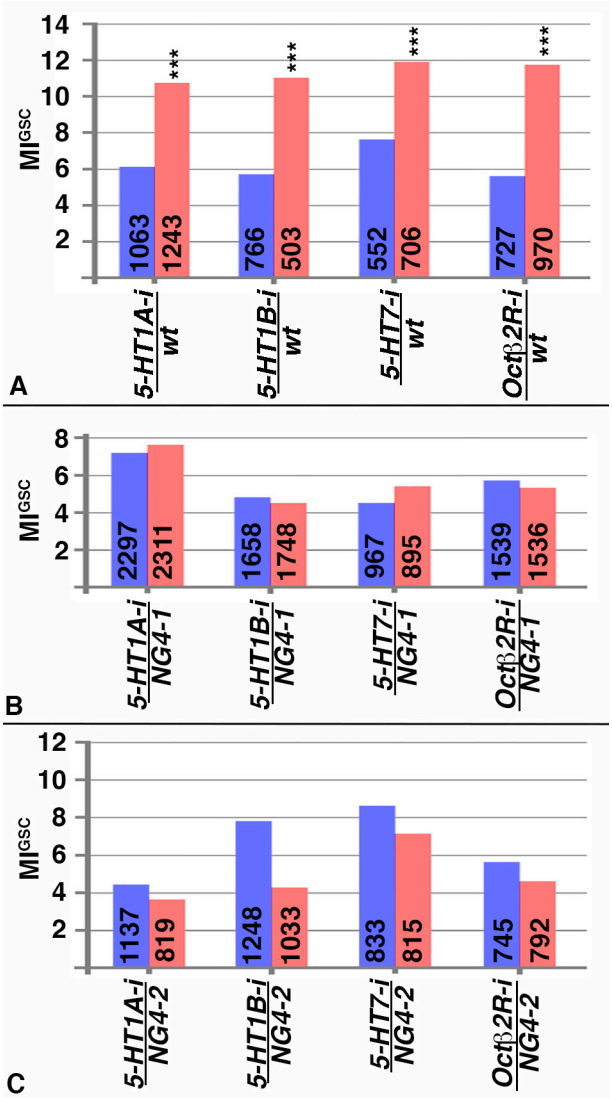
A
MI GSC
14
12
10
8
6
4
2
1063
1243
766
503
552
706
727
970
***
***
***
***
5-HT1A-i / wt
5-HT1B-i / wt
5-HT7-i / wt
Octβ2R-i / wt
B
MI GSC
8
6
4
2
2297
2311
1658
1748
967
895
1539
1536
5-HT1A-i / NG4-1
5-HT1B-i / NG4-1
5-HT7-i / NG4-1
Octβ2R-i / NG4-1
C
MI GSC
12
10
8
6
4
2
1137
819
1248
1033
833
815
745
792
5-HT1A-i / NG4-2
5-HT1B-i / NG4-2
5-HT7-i / NG4-2
Octβ2R-i / NG4-2

**Figure 3**

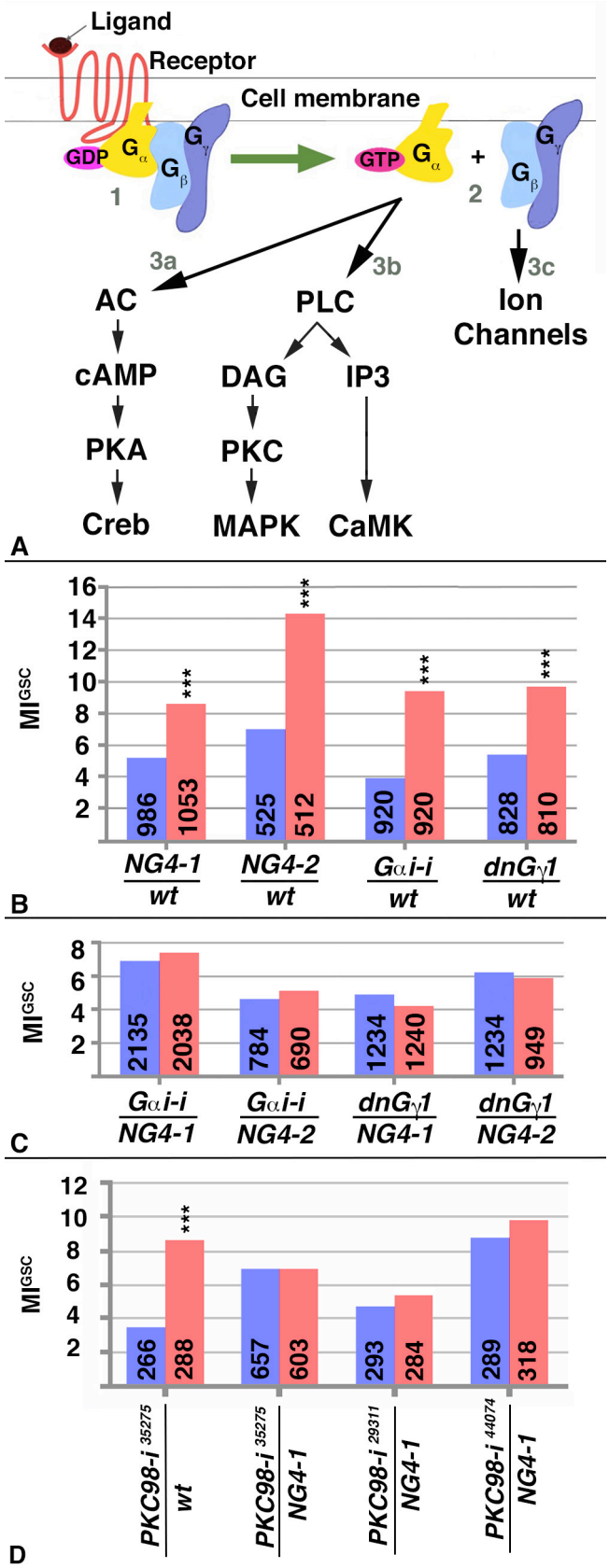
Ligand
Receptor
Cell membrane
GDP
Gα
Gβ
Gγ
1
GTP
Gα
+
2
Gβ
Gγ
3a
3b
3c
AC
PLC
Ion Channels
cAMP
DAG
IP3
PKA
PKC
Creb
MAPK
CaMK
A
MI^GSC
986
1053
525
512
920
920
828
810
NG4-1 wt
NG4-2 wt
Gαi-i wt
dnGγ1 wt
B
2135
2038
784
690
1234
1240
1234
949
Gαi-i NG4-1
Gαi-i NG4-2
dnGγ1 NG4-1
dnGγ1 NG4-2
C
266
288
657
603
293
284
289
318
PKC98-i 35275 wt
PKC98-i 35275 NG4-1
PKC98-i 29311 NG4-1
PKC98-i 44074 NG4-1
D

**Figure 4**

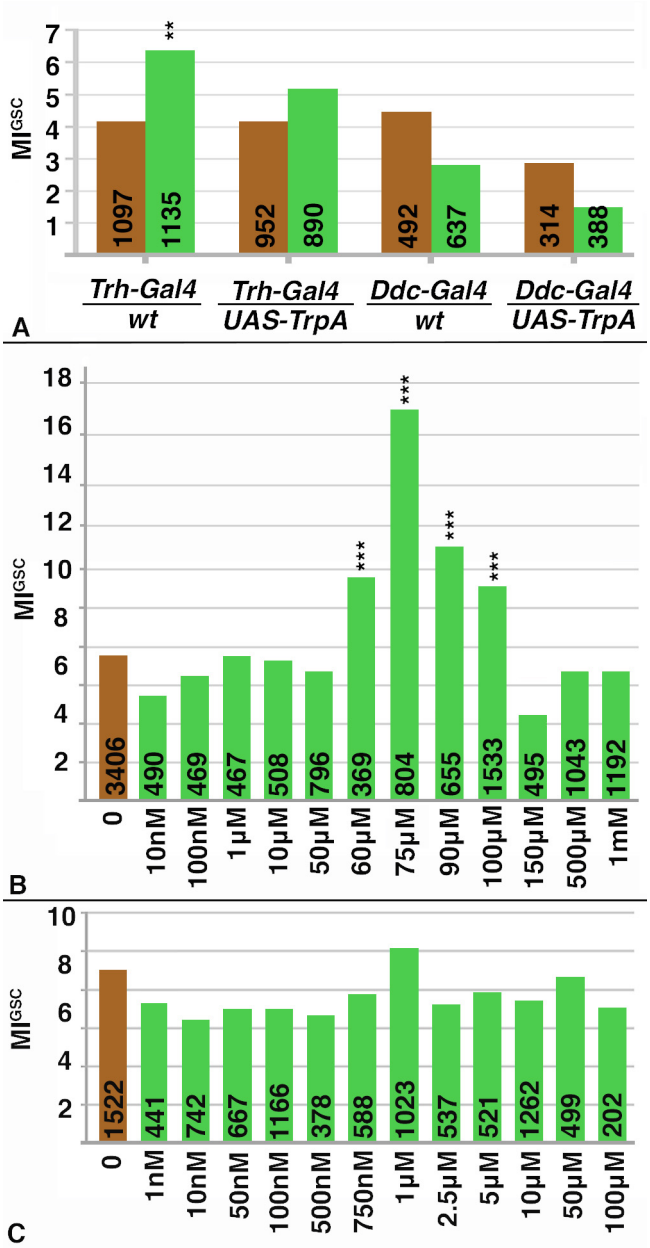
A
MI^GSC
7
6
5
4
3
2
1
**
1097
1135
952
890
492
637
314
388
Trh-Gal4 wt
Trh-Gal4 UAS-TrpA
Ddc-Gal4 wt
Ddc-Gal4 UAS-TrpA
B
MI^GSC
18
16
14
12
10
8
6
4
2
***
***
***
3406
490
469
467
508
796
369
804
655
1533
495
1043
1192
0
10nM
100nM
1µM
10µM
50µM
60µM
75µM
90µM
100µM
150µM
500µM
1mM
C
MI^GSC
10
8
6
4
2
1522
441
742
667
1166
378
588
1023
537
521
1262
499
202
0
1nM
10nM
50nM
100nM
500nM
750nM
1µM
2.5µM
5µM
10µM
50µM
100µM

**Figure 5**

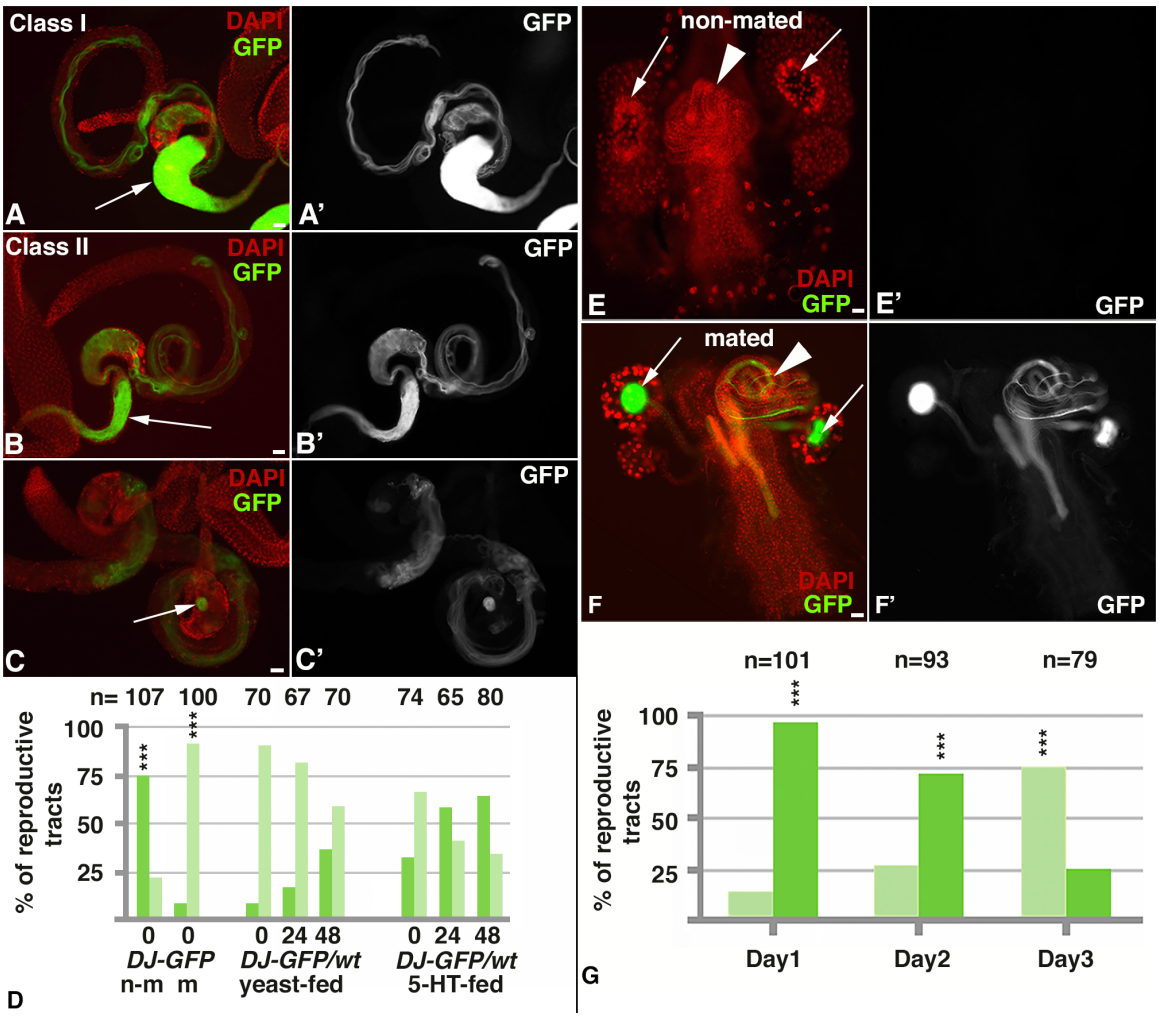
Class I
DAPI
GFP
A
GFP
A'
Class II
DAPI
GFP
B
GFP
B'
DAPI
GFP
C
GFP
C'
non-mated
DAPI
GFP
E
E'
GFP
mated
DAPI
GFP
F
F'
GFP
n= 107 100 70 67 70 74 65 80
% of reproductive tracts
100
75
50
25
***
***
0 0 0 24 48 0 24 48
DJ-GFP
n-m m
DJ-GFP/wt
yeast-fed
DJ-GFP/wt
5-HT-fed
D
n=101 n=93 n=79
% of reproductive tracts
100
75
50
25
***
***
***
Day1
Day2
Day3
G

**Figure 6**

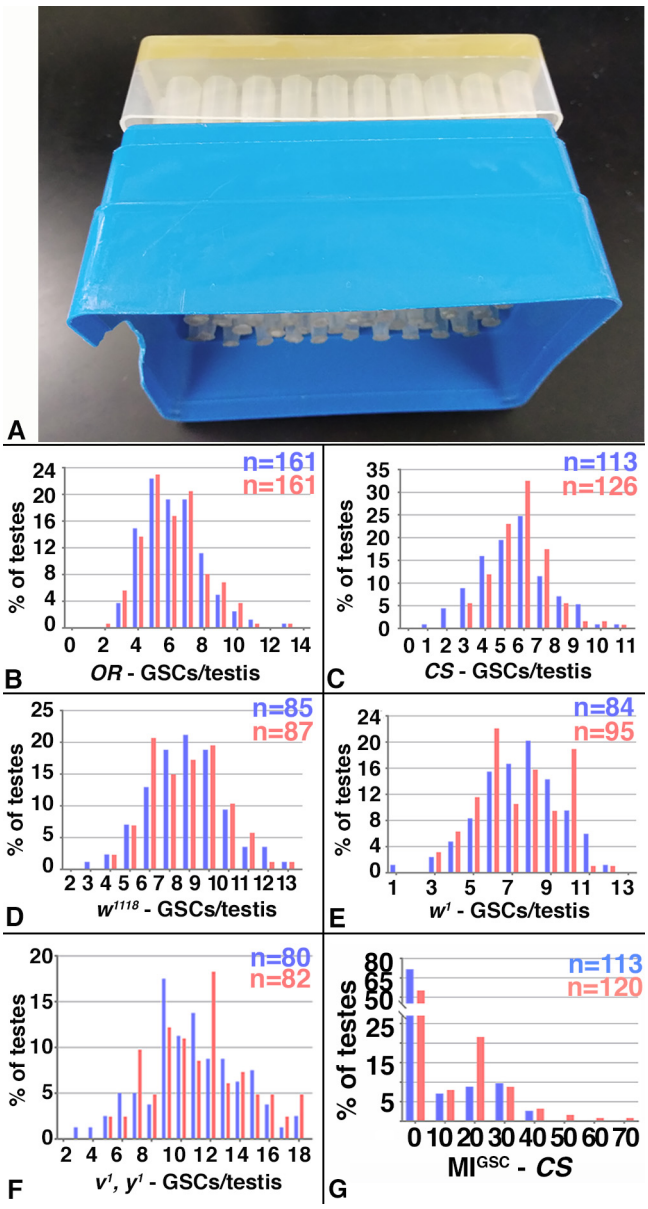
A
n=161
n=161
% of testes
OR - GSCs/testis
B
n=113
n=126
% of testes
CS - GSCs/testis
C
n=85
n=87
% of testes
w1118 - GSCs/testis
D
n=84
n=95
% of testes
w1 - GSCs/testis
E
n=80
n=82
% of testes
v1, y1 - GSCs/testis
F
n=113
n=120
% of testes
MIGSC - CS
G

**Figure S1**

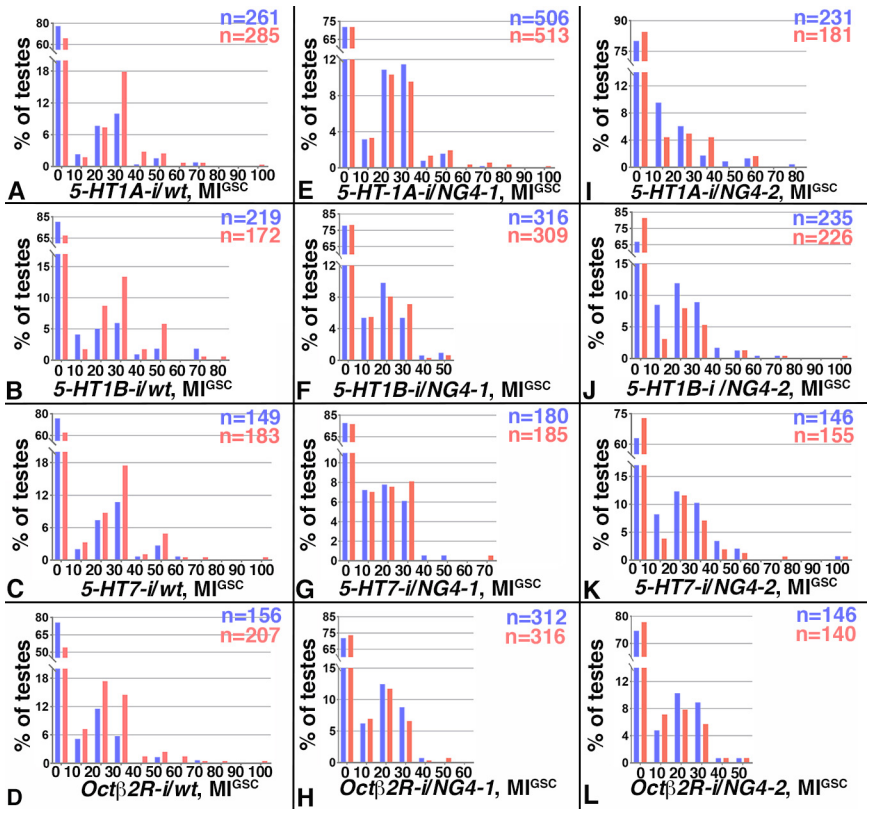
A
5-HT1A-i/wt, MI^GSC
n=261
n=285
B
5-HT1B-i/wt, MI^GSC
n=219
n=172
C
5-HT7-i/wt, MI^GSC
n=149
n=183
D
Octβ2R-i/wt, MI^GSC
n=156
n=207
E
5-HT-1A-i/NG4-1, MI^GSC
n=506
n=513
F
5-HT1B-i/NG4-1, MI^GSC
n=316
n=309
G
5-HT7-i/NG4-1, MI^GSC
n=180
n=185
H
Octβ2R-i/NG4-1, MI^GSC
n=312
n=316
I
5-HT1A-i/NG4-2, MI^GSC
n=231
n=181
J
5-HT1B-i /NG4-2, MI^GSC
n=235
n=226
K
5-HT7-i/NG4-2, MI^GSC
n=146
n=155
L
Octβ2R-i/NG4-2, MI^GSC
n=146
n=140
% of testes

**Figure S2**

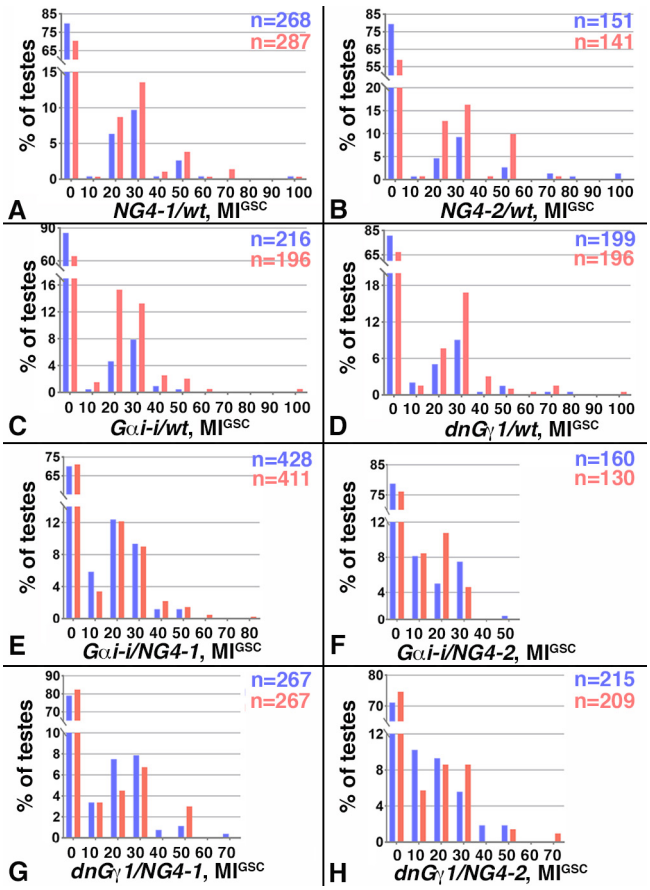
A
% of testes
n=268
n=287
NG4-1/wt, MI^GSC
B
% of testes
n=151
n=141
NG4-2/wt, MI^GSC
C
% of testes
n=216
n=196
Gαi-i/wt, MI^GSC
D
% of testes
n=199
n=196
dnGγ1/wt, MI^GSC
E
% of testes
n=428
n=411
Gαi-i/NG4-1, MI^GSC
F
% of testes
n=160
n=130
Gαi-i/NG4-2, MI^GSC
G
% of testes
n=267
n=267
dnGγ1/NG4-1, MI^GSC
H
% of testes
n=215
n=209
dnGγ1/NG4-2, MI^GSC

**Figure S3**

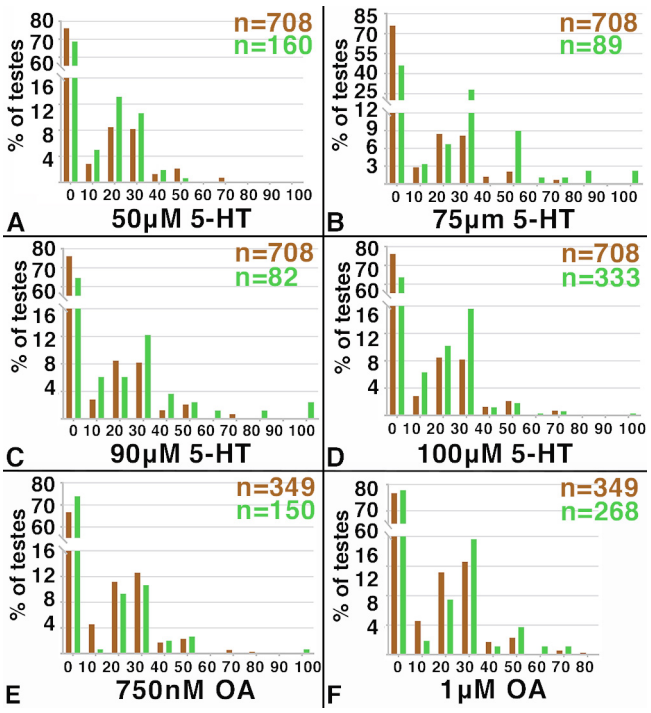
A
50µM 5-HT
n=708
n=160
% of testes
B
75µm 5-HT
n=708
n=89
C
90µM 5-HT
n=708
n=82
D
100µM 5-HT
n=708
n=333
E
750nM OA
n=349
n=150
F
1µM OA
n=349
n=268

**Figure S4**